THE JOURNAL OF BIOLOGICAL CHEMISTRY VOL. 286, NO. 5, pp. 3418–3428, February 4, 2011

Transactivation of the Epidermal Growth Factor Receptor by Heat Shock Protein 90 via Toll-like Receptor 4 Contributes to the Migration of Glioblastoma Cells*[S]

Received for publication, June 15, 2010, and in revised form, December 1, 2010 Published, JBC Papers in Press, December 2, 2010, DOI 10.1074/jbc.M110.154823

Dominique Thuringer[‡1], Arlette Hammann[‡], Naïma Benikhlef[‡], Eric Fourmaux[‡], André Bouchot[§], Guillaume Wettstein[‡], Eric Solary[‡¶], and Carmen Garrido[‡]

From the [‡]INSERM U866 and [§]Cell Imaging Platform IFR100, Faculty of Medicine, 7 Boulevard Jeanne d'Arc, 21000 Dijon and the [¶]INSERM U1009, Institut Gustave Roussy, Avenue Camille Desmoulins, 95008 Villejuif, France

Extracellular heat shock protein HSP90α was reported to participate in tumor cell growth, invasion, and metastasis formation through poorly understood signaling pathways. Herein, we show that extracellular HSP90α favors cell migration of glioblastoma U87 cells. More specifically, externally applied HSP90α rapidly induced endocytosis of EGFR. This response was accompanied by a transient increase in cytosolic Ca^{2+} appearing after 1–3 min of treatment. In the presence of EGF, U87 cells showed HSP90α-induced Ca^{2+} oscillations, which were reduced by the ATP/ADPase, apyrase, and inhibited by the purinergic P_2 inhibitor, suramin, suggesting that ATP release is requested. Disruption of lipid rafts with methyl β-cyclodextrin impaired the Ca^{2+} rise induced by extracellular HSP90α combined with EGF. Specific inhibition of TLR4 expression by blocking antibodies suppressed extracellular HSP90α-induced Ca^{2+} signaling and the associated cell migration. HSPs are known to bind lipopolysaccharides (LPSs). Preincubating cells with Polymyxin B, a potent LPS inhibitor, partially abrogated the effects of HSP90α without affecting Ca^{2+} oscillations observed with EGF. Extracellular HSP90α induced EGFR phosphorylation at Tyr-1068, and this event was prevented by both the protein kinase Cδ inhibitor, rottlerin, and the c-Src inhibitor, PP2. Altogether, our results suggest that extracellular HSP90α transactivates EGFR/ErbB1 through TLR4 and a PKCδ/c-Src pathway, which induces ATP release and cytosolic Ca^{2+} increase and finally favors cell migration. This mechanism could account for the deleterious effects of HSPs on high grade glioma when released into the tumor cell microenvironment.

Glioma ranges from slowly growing low grade tumors to rapidly growing high grade tumors, including anaplastic astrocytoma and glioblastoma (1, 2). High grade gliomas include anaplastic tumor cells, necrotic foci, and rich vascularity, due largely to the aberrant expression of angiogenic factors by tumor cells (3). Tumor cells are highly proliferative and invasive within the brain. Despite the development of various treatments, the life expectancy of patients remains poor (4).

One of the molecules that could contribute to invasion is the stress or heat shock protein 90 (HSP90). In several tumor types, cell surface expression of HSP90 correlates with metastatic potential (5), and its inhibition with antibodies (6, 7) or with cell-impermeable inhibitors (8) reduces cell migration *in vitro*. Of the two HSP90 isoforms, only HSP90α has been described extracellularly, which argues against cell lysis as the source of extracellular HSP90 (8). The metalloprotease MMP-2 can be associated with extracellular HSP90α (8), which is favored by acetylation of the stress protein (9). Surface HSP90α also participates in extracellular matrix protein-induced c-Src/integrin association and reorganization of the actin cytoskeleton (10). The cell-impermeable inhibitor of HSP90, 17-dimethylaminoethylamino-17-demethoxygeldanamycin (DMAG)-*N*-oxide, displays anti-invasive and anti-metastatic activity *in vitro* and *in vivo*, respectively, probably through the inhibition of actin polymerization and focal adhesion formation (11). Actin polymerization can be activated by tyrosine kinase receptors of the EGFR[2] family (12). Cell surface HSP90α interacts specifically with the extracellular domain of HER-2 (also known as ErbB2), a ligand-less receptor, forming heterodimers with ligand-bound members ErbB1 (EGFR), ErbB3, and ErbB4. The HSP90α/HER-2 interaction favors HER-2 heterodimerization with ErbB3 and signal transduction pathways via MAPK and PI3K-Akt, leading to actin rearrangement and cell motility (7). EGFR (ErbB1, or HER1) is overexpressed in 60% of multiform glioblastomas (13, 14) and promotes invasion, proliferation, and metastasis (15–17) in response to several ligands known as EGF-related peptide growth factors (18). Binding of these ligands to the extracellular domain of EGFR leads to the formation of homo- and heterodimers, which triggers autophosphorylation of specific tyrosine residues within the cytoplasmic domain of EGFR, inducing signaling cascades. Ligand-independent EGFR activation, referred to as EGFR transactivation, can also be observed in response to various agents such as Toll-Like receptor (TLR) agonists and stress conditions (19, 20).

* This work was supported by grants from the CNRS, INSERM, and by Conseil Régional de Bourgogne (CRB, Faber Program) and by grants from are supported by the Ligue Nationale Contre le Cancer (to E. S. and C. G.).

[S] The on-line version of this article (available at http://www.jbc.org) contains supplemental Figs. S1–S8.

[1] To whom correspondence should be addressed. Tel.: 33-3-80-39-34-17; Fax: 33-3-80-39-34-34; E-mail: dominique.thuringer@u-bourgogne.fr.

[2] The abbreviations used are: EGFR, epidermal growth factor receptor; TLR, Toll-like receptor; TSG, thapsigargin; MβCD, methyl-β-cyclodextrin; HB, heparin binding; MMP, matrix metalloproteinase; ER, endoplasmic reticulum; P, phospho; HC, heavy chain; ADAM, a disintegrin and metalloproteinase.

The aim of this study was to investigate the role of extracellular HSP90α in signaling events triggered by EGFR in the human astrocytoma cell line (U87). We show that exogenously applied HSP90α mediates a cross communication between TLR4 and EGFR and accelerates cell migration.

EXPERIMENTAL PROCEDURES

Cell Culture—Human astrocytoma cell line (U87-MG; European Collection of Cell Cultures, Sigma-Aldrich) was grown in Dulbecco's modified Eagle's medium (DMEM) plus 10% fetal bovine serum (Lonza) (5% CO_2; 37 °C). Cells were incubated 12–24 h in serum-free culture medium before use.

Materials—Rabbit polyclonal anti-HSP90α and anti-HSP70 antibodies were purchased from Affinity Bioreagents. Human recombinant HSP90α protein was from StressGen (assay designs) and from BPS Bioscience. Neutralizing anti-TLR4, mouse monoclonal anti-TLR4, and rat monoclonal anti-EGFR (ErB1) antibodies were from Abcam (Cambridge, UK). Rabbit monoclonal anti-P-EGFR (Tyr-1068) and antibodies to phospho- and total SAPK/JNK (Tyr-183/185), NFκB p65 (Ser-536), IRF-3 (Ser-396), Akt (Ser-473), and p44/p42 MAPK (Thr-202/204) were purchased from Cell Signaling Technology. Goat polyclonal clathrin-HC-FITC and mouse monoclonal caveolin-1-FITC were purchased from Santa Cruz Biotechnology. The antibody to proHB-EGF was purchased from R&D Systems Inc. Human recombinant EGF, LPSs from *Escherichia coli*, fura-2-acetometoxymethyl ester (fura-2/AM), Alexa Fluor dye conjugates, phalloidin, and secondary antibodies were from Molecular Probes. Human TLR4 shRNA, EGFR (ErbB1), and control lentiviral particles purchased from Santa Cruz Biotechnology. HER2 (ErbB2) tyrosine kinase inhibitor (Gefitinib) was provided by AstraZeneca. The phospholipase C inhibitor (U73122), the protein kinase C (PKC) inhibitor (bisindolylmaleimide), the specific PKCδ inhibitor (rottlerin), the c-Src kinase-specific inhibitor (4-amino-5-(4-chlorophenyl)-7-(*t*-butyl)pyrazolo[3,4-D]pyrimidine, PP2) and its inactive isomer (4-amino-7-phenylpyrazolo[3,4-D]pyrimidine, PP3), EGFR (ErbB1) tyrosine kinase inhibitor (tyrphostin AG1478), galardin (GM6001), diphtheria toxin mutant (CRM197), and specific inhibitor of endoplasmic reticulum Ca^{2+}-ATPases (thapsigargin (TSG)) were purchased from Calbiochem. The IκBα/NFκB-p65 phosphorylation inhibitor, (E)-3-[4-methyl-phenylsulfonyl]-2-proprenenitrile (BAY11-7082), was purchased from Santa Cruz Biotechnology. Other chemicals were obtained from Sigma.

Specific Cell Treatments—EGF was used at a unique dose of 10 ng/ml. To rule out the possible implication of HER2 in EGF-induced cell responses, 5 μM gefitinib was added. For cholesterol depletion, cells were incubated for 30–60 min at 37 °C in serum-free medium containing 0.1% bovine serum albumin (BSA) and 7.5 mM methyl-β-cyclodextrin (MβCD), a mixture known to reduce plasma membrane cholesterol levels with no cell death (21). Cells were preincubated with Polymyxin B, a potent LPS inhibitor (10 μM; 30–60 min), to avoid bacterial contamination of HSP90α before activation. An additional control was to boil HSP90α at 100 °C for 1 h to suppress the specific effect of HSP90α because LPSs are resistant to heat inactivation but not HSPs (22–24).

Immunofluorescence Experiments—Cells were fixed in 4% paraformaldehyde and permeabilized with 0.1% Triton X-100. Cells were incubated with the primary antibody for 2 h and then secondary antibody (F(ab′)2 fragment of IgG) conjugated with Alexa Fluor 488 nm or 568 nm (1:500) or with Alexa Fluor 488-conjugated phalloidin for 30 min. Substituting the primary antibody with preimmune serum demonstrates specificity of labeling. Counterstaining of nuclei was made using 40,6-diamidino-2-phenylindole (DAPI; 3 μg/ml, 1–3 min). Images were collected on Axioplan 2 microscope using Axiovision Viewer 3 software (Zeiss). The intensity of labeled area (10 μm^2) was measured with ImageJ analysis software. In some experiments, imaging was performed with a Leica SP2 RS confocal microscope, and Z-series of optical sections taken from 0.4-μm intervals were collected using the scanning format 1024 × 1024 pixels.

Flow Cytometry—Flow cytometry was carried out using the LSRII and FlowJO software. Briefly, cells were washed twice with PBS containing 1% BSA and stained with primary antibodies (1:200 to 1:100, 1 h at 4 °C) and then with Alexa Fluor-conjugated secondary antibodies (1:1000; 30 min at 4 °C; Molecular Probes).

Cytosolic Free Ca^{2+} Concentration—Changes in Fura-2 fluorescence were used to measure $[Ca^{2+}]_i$. Briefly, confluent cells were incubated with 2 μM fura-2-acetometoxymethyl ester in culture medium (40 min at 37 °C) and then in HEPES-buffered saline solution containing in mM: 120 NaCl, 5.4 KCl, 0.8 $MgCl_2$, 10 glucose, and 20 HEPES, pH 7.4. In nominally Ca^{2+}-free conditions, no $CaCl_2$ addition was made. Dimethyl sulfoxide (DMSO) or ethanol, used to dissolve drug, was added in other solutions. Measurements were made on an inverted microscope (Nikon TS100) equipped with a 20× objective (Nikon S Fluor, 0.75 NA) attached to a dual-excitation spectrofluorometer with excitation wavelengths alternating between 340 and 380 nm. Emission fluorescence (510 nm) was collected at a rate of 20/min. The 340/380 nm ratio was determined for each cell, and average values were reported as a function of time.

ATP Assay—Cells were exposed to HSP90α and/or EGF, and then the supernatants were collected to assess the amount of ATP release with luciferin-based ENLITEN ATP assay (Promega) at various time periods. Briefly, 100 μl of luciferin-luciferase solution were added to supernatants, and light emission was recorded with a FLUOstar luminometer (BMG LABTECH). We calibrated light emission by using standard samples furnished by the manufacturer.

Internalization Assay—Cells were incubated with 200 μg/ml anti-HSP90 for various time periods from 5 min to 2 h and then washed and fixed in paraformaldehyde. To detect possible internalization of anti-HSP90 antibody, permeabilized cells were incubated with Alexa Fluor 488-conjugated secondary antibody. For endocytosis analysis, cells were incubated 15 min in HEPES-buffered saline solution with $CaCl_2$ before experiment. The control solution containing 5 μM BSA-Alexa Fluor 568 was applied 15 min to attest the absence of nonspecific endocytosis. EGF-BSA-Alexa Fluor 488 or BSA-Alexa Fluor 568 (1:20) were applied for 15 min (about 20

nM EGF) with or without HSP90α. Cells were post-fixed and mounted on slides to be analyzed.

Immunodetection of Protein Phosphorylation—Cell monolayers were washed five times with ice-cold PBS and lysed (45 min on ice) using 1 ml of lysis buffer containing: 50 mM Tris-HCl, pH 7.4, 1% Nonidet P-40, 0.25% sodium deoxycholate, 150 mM NaCl, 1 mM EGTA, 1 mM NaF, 100 μM sodium orthovanadate, 100 μM phenylmethylsulfonyl fluoride, and protease inhibitor mixture (Roche Applied Science). Cells were scraped and centrifuged, and lysates were collected. Proteins were boiled for 5 min in 2 μl of SDS buffer, fractionated using 8% SDS-PAGE, and transferred to nitrocellulose membranes (Bio-Rad). Membranes were blocked for 1 h with 5% BSA in Tris-buffered saline with Tween 20 (0.1%) (TBS-T) and incubated overnight with antibodies. For EGFR phosphorylation, proteins (20–60 μg/lane) were immunoblotted with anti-P-EGFR (1:50) and revealed with ECL reagents (Amersham Biosciences). Membrane was stripped and reprobed with antibody against EGFR to evaluate the total amount of EGFR.

Wound Healing Migration—A 1-mm-wide cell-free area was generated by gently scratching the cell monolayer with a sterile yellow Gilson pipette tip. The recording DMEM containing drugs or specific antibodies was applied (5% CO_2 in air at 37 °C). Migration of astrocytes within the gap was monitored at given time intervals, using a Zeiss microscope equipped with a video camera. The extent of healing was defined as the ratio of denuded areas of the original wound and the wound after 11–22 h.

Bromodeoxyuridine Incorporation Assay—Serum-starved U87 cells cultured in the presence or absence of agents were exposed to bromodeoxyuridine at a concentration of 3 mM for 1 h. Cells were subsequently rinsed and fixed in 70% ethanol overnight, then washed and reincubated for another 10 min in 2 M HCl containing 0.1% Triton X-100 followed by a 20-min incubation in 0.1 M sodium borate. Cells were processed for immunofluorescence using an anti-bromodeoxyuridine antibody (Dako) and an appropriate Alexa Fluor 488-conjugated secondary antibody.

Statistical Analysis—One-way analysis of variance (Statview Software) was used to compare data groups. p values < 0.05 were significant.

RESULTS

Extracellular HSP90α Accelerates Glioblastoma Cell Migration in Vitro—Immunofluorescence analyses detected the HSP90α isoform at the cell surface of glioblastoma U87 cells (Fig. 1*A*). HSP90α isoform was mainly expressed at the front edge of migration of cells. The extracellular localization of HSP90α was confirmed by flow cytometry. In contrast, no HSP70 was detected at the cell surface (Fig. 1*A*, *right panel*). To analyze the cellular basis for the invasive effect of extracellular HSP90α, we used a wound healing assay. The addition of recombinant HSP90α protein to serum-free medium enhanced cell invasion in a dose-dependent manner (*i.e.* in the range from 60 ng/ml to 6 μg/ml). This resulted in higher rates of gap closure observed as early as the first hour of cell incubation and confirmed in the following hours, 6 and 12 h (Fig. 1*B*). It is worthy to note that the effect of HSP90α is directed more toward cell migration than toward cell proliferation because a lower percentage of bromodeoxyuridine incorporation was observed (Fig. 1*B*, *table*). For instance, cell proliferation and invasion were respectively increased by 5 ± 1 and 15 ± 2% from control values following 6 h of cell exposure to 6 μg/ml HSP90α. Such an increase in cell migration was also observed with 10 ng/ml EGF and amplified by the combination of the two molecules (Fig. 1*C*). An additive effect of the activation of cell invasion was observed when both agents were added together into the cell bath medium. These results suggested that extracellular HSP90α exerted an additive effect on the ability of EGF to promote U87 cell migration.

Extracellular HSP90α Increases $[Ca^{2+}]_i$ in U87 Cells—To determine the role of Ca^{2+} store in U87 response to HSP90α, we measured $[Ca^{2+}]_i$, in the presence and absence of extracellular calcium, in fura-2-loaded cells. Recombinant HSP90α induced a transient increase in $[Ca^{2+}]_i$ within 1–3 min (Fig. 2*A*, *left panel*), whereas EGF induced a more sustained biphasic calcium response with a rapid peak followed by a plateau phase (Fig. 2*A*, *right panel*). In a few experiments, the agonist was applied in the absence of external Ca^{2+} to reveal release from internal stores. Then, Ca^{2+} was restored extracellularly to reveal increase in plasma membrane Ca^{2+} permeability (Fig. 2*B*). A subsequent application of 2 μM TSG was made at the end of some recordings to estimate the Ca^{2+} content of intracellular endoplasmic reticulum (ER) pools. In nominally Ca^{2+}-free conditions, 6 μg/ml HSP90α induced a transient Ca^{2+} release from intracellular pools (Fig. 2*B*, *left panel*). The addition of Ca^{2+} to the bath medium did not induce a significant increase in $[Ca^{2+}]_i$, whereas TSG drastically increased $[Ca^{2+}]_i$ in the absence of external Ca^{2+}, demonstrating that HSP90α did not deplete completely internal stores. In Ca^{2+}-free conditions, the amplitude of Ca^{2+} peak induced by EGF remained unchanged, but the duration of the plateau phase was decreased, and Ca^{2+} readdition to the bath medium resulted in a transient Ca^{2+} influx through plasma membrane channels due to capacitative Ca^{2+} entry (Fig. 2*B*, *right panel*). Upon stimulation with EGF, the cells showed calcium oscillations in response to HSP90α (*i.e.* with a frequency of three spikes per 5 min; 98%, $n = 50$), which were rapidly abolished by the removal of HSP90α (Fig. 2*C*) or the addition of the EGFR/ErbB1 inhibitor Tyrphostin (AG1478), whereas the addition of ErbB2 inhibitor Gefitinib had no effect (supplemental Fig. S2). These results suggested that HSP90α could promote calcium oscillation through EGFR/ErbB1.

ADP/ATP Contributes to HSP90α-induced $[Ca^{2+}]_i$ Rise in Glioblastoma Cells—To determine whether the calcium oscillatory process elicited by HSP90α and EGF may involve the release of ATP/ADP and their interaction with purinergic (P2) receptors (25, 26), we pretreated U87 cells with the P2 receptor antagonist suramin (10 μM for 10 min) and the extracellular ATP scavenger apyrase (40 units/ml for 10 min). Both compounds drastically attenuated Ca^{2+} oscillations generated by exogenously added EGF plus HSP90α (Fig. 2*C*, *right panel*). To assess the effect of HSP90α and EGF on the subsequent ATP release, cells were exposed to these agents for various periods of time (from 15 min to 1, 6, and 12 h), and supernatants were collected to evaluate amounts of ATP by

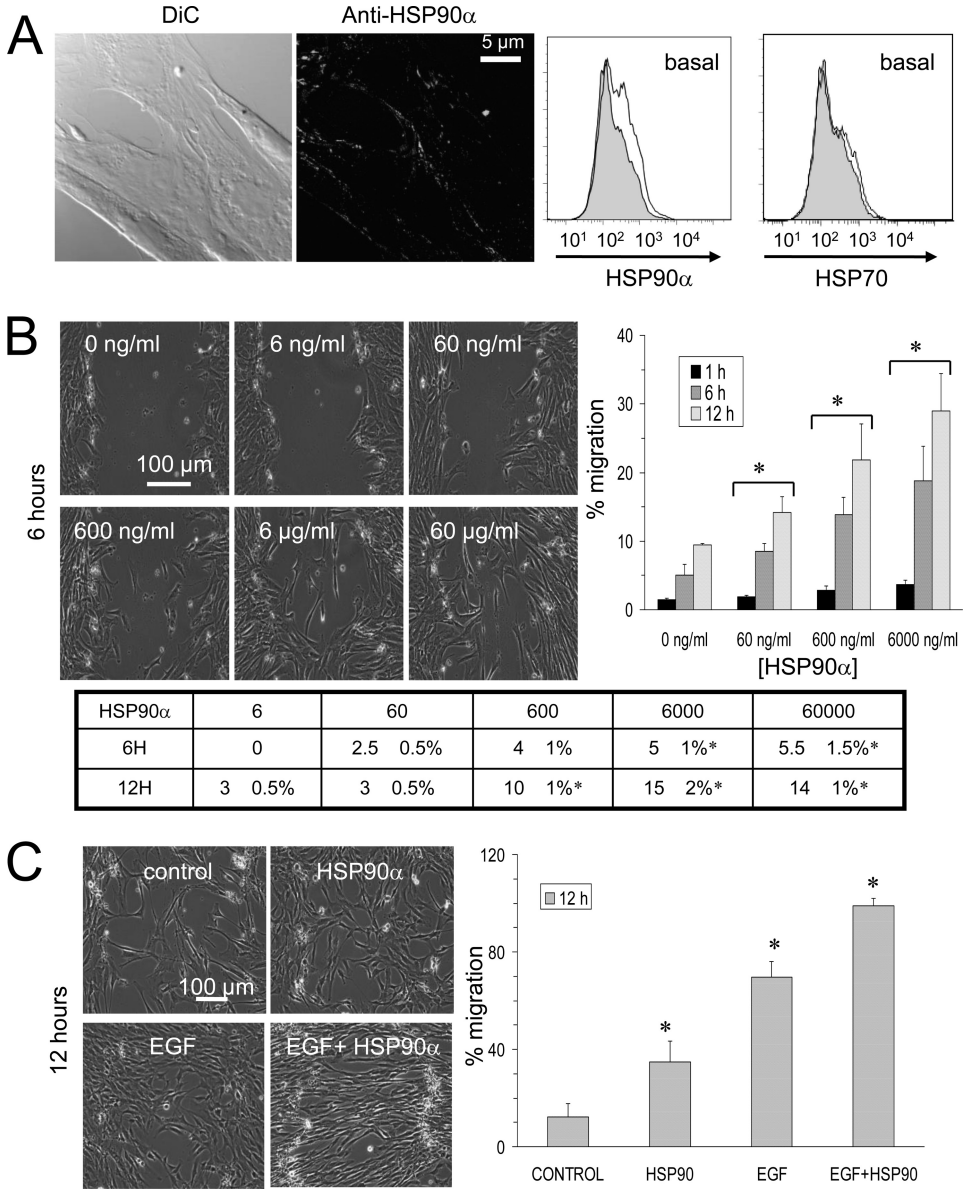

HSP90α	6	60	600	6000	60000
6H	0	2.5 0.5%	4 1%	5 1%*	5.5 1.5%*
12H	3 0.5%	3 0.5%	10 1%*	15 2%*	14 1%*

FIGURE 1. **Extracellular HSP90α amplifies EGF-induced cell motility and cytoskeletal rearrangement of astroglioma U87 cells.** *A*, cell surface expression of HSP90α. Immunofluorescence labeling of U87 cells using anti-HSP90α and an additional signal amplification step (biotin/streptavidin Alexa Fluor 488) indicates the surface pool of HSP90α. Confocal optical section of 0.4 μm thickness is shown ($n = 6$ experiments). The extracellular localization of HSP90α was confirmed by flow cytometry analysis using anti-HSP90α or anti-HSP70 (*white histograms*) compared with isotype IgG (*gray filled histograms*) ($n = 3$). *DiC*, differential interference contrast. *B*, dose-dependent effect of extracellular HSP90α on cell migration after 1, 6, and 12 h of cell exposure. The table shows the relative values (percentage of control) of the bromodeoxyuridine incorporation in U87 cells after exposure to increasing doses of HSP90α (ng/ml) for 6 or 12 h (mean ± S.D., $n = 2$; *, p values<0.05 *versus* control). *C*, quantitative effect of HSP90α (6 μg/ml) and/or EGF (10 ng/ml) on the closure of wound depicted in the histogram after 12 h of cell treatment (mean ± S.D., $n = 3$; *, p values<0.05 *versus* control).

bioluminescence assay (Fig. 2*D*). Clearly no significant release of ATP could be detected in the absence or presence of HSP90α. In contrast, HSP90α plus EGF released ATP from U87 cells to a higher extent than did EGF alone within the first 15–30 min of cell stimulation. Altogether, EGF triggers Ca^{2+} oscillations that are amplified by extracellular HSP90α through release of ATP acting on purinergic P2 receptors.

Extracellular HSP90α Induces EGFR Internalization and Tyrosine Phosphorylation—Cell exposure to HSP90α for 15 min markedly reduced EGFR surface expression (Fig. 3*A*). U87 cells were incubated in the presence of BSA-Alexa Fluor 568, a membrane-impermeable macromolecule, before adding HSP90α for 15 min and then staining permeabilized cells. Green EGFR was identified at the cell periphery and in the juxtanuclear region (Fig. 3*B*). In HSP90α-stimulated cells, BSA co-localized with EGFR in the juxtanuclear region, suggesting a rapid internalization (Fig. 3*B*). Pretreatment with MβCD to deplete cholesterol and disrupt lipid raft organization prevented the calcium response to HSP90α in the absence or presence of EGF, suggesting that lipid raft integrity may be essential for HSP90α-induced Ca^{2+} signaling (Fig. 3*C*). Cell exposure to HSP90α did not change significantly the level of ErbB1 *versus* total EGFR proteins (not shown). Both EGF and HSP90α induced EGFR phosphorylation at Tyr-1068 within 15 min, which was attenuated by cell pretreatment with the PKCδ inhibitor, rottlerin (Fig. 4*A*). Because PKC

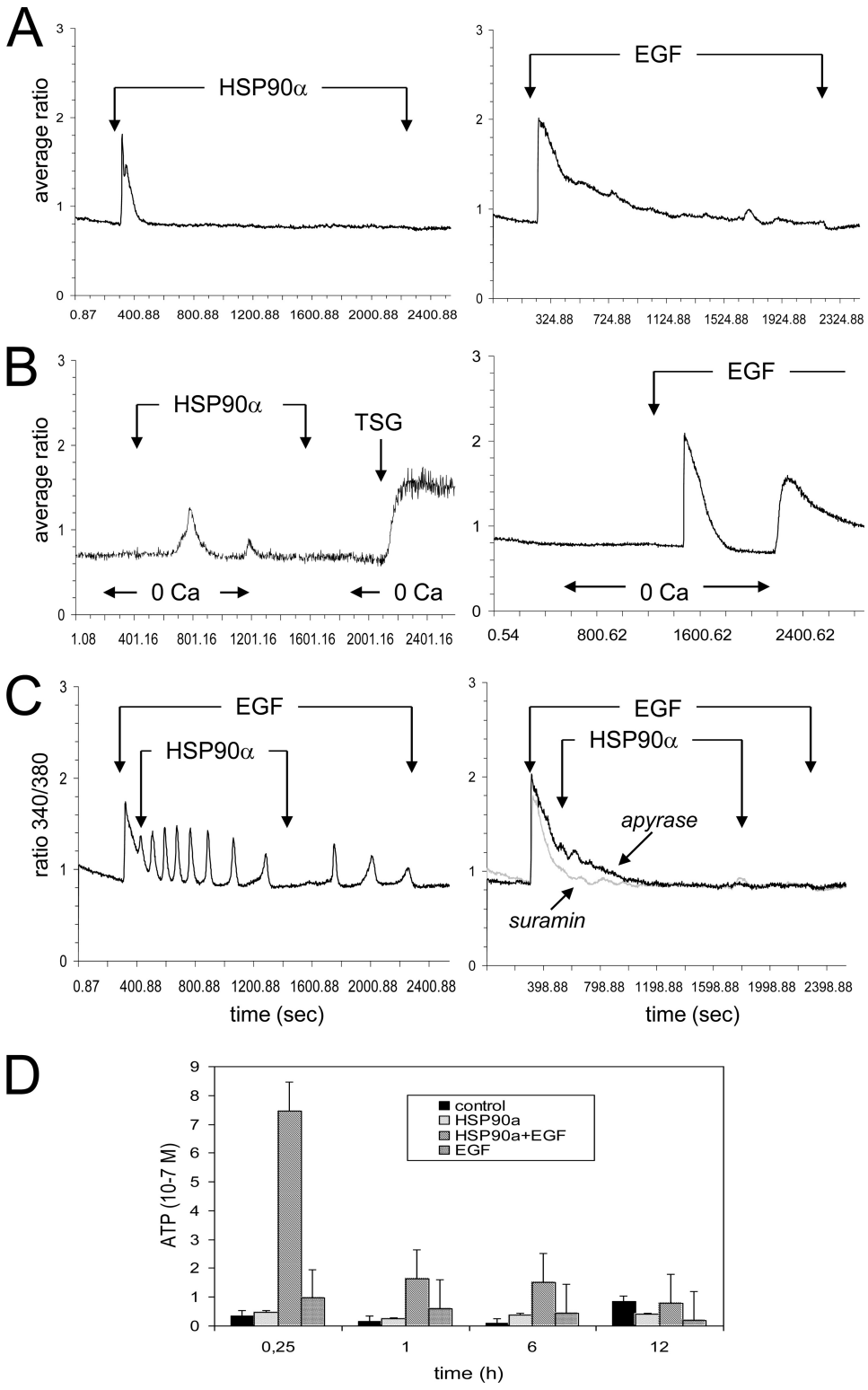

FIGURE 2. **Extracellular HSP90α induces Ca^{2+} mobilization in astroglioma U87 cells.** *A*, the additions of HSP90α or EGF are indicated by the *arrow* (average of 10 cells; $n = 10$). *B*, HSP90α-induced intracellular Ca^{2+} release from internal stores. Changes in bathing conditions (0 mM $CaCl_2$) are indicated on the bottom of traces. HSP90α or EGF was initially applied in the absence and then the presence of external Ca^{2+} (1.8 mM) to reveal Ca^{2+} release from internal stores and external Ca^{2+} entry, respectively (average of 20 cells). 2 μM TSG was tested at the end of recording. *C*, HSP90α induced an oscillatory Ca^{2+} process during EGF-induced Ca^{2+} plateau ($n = 10$). The *right panel* shows the contribution of ATP-mediated pathways to HSP90α-induced Ca^{2+} signaling in superimposed traces obtained from cells preincubated with apyrase (40 units/ml) or suramin (10 μM) for 10 min, before the addition of HSP90α plus EGF ($n = 10$). *D*, ATP release into the supernatant of U87 cells treated with HSP90α and/or EGF for various periods of time as indicated. The amounts of external ATP were measured with a luciferin-based ENLITEN ATP assay. Means ± S.D. of triplicates of one representative experiment out of three are depicted.

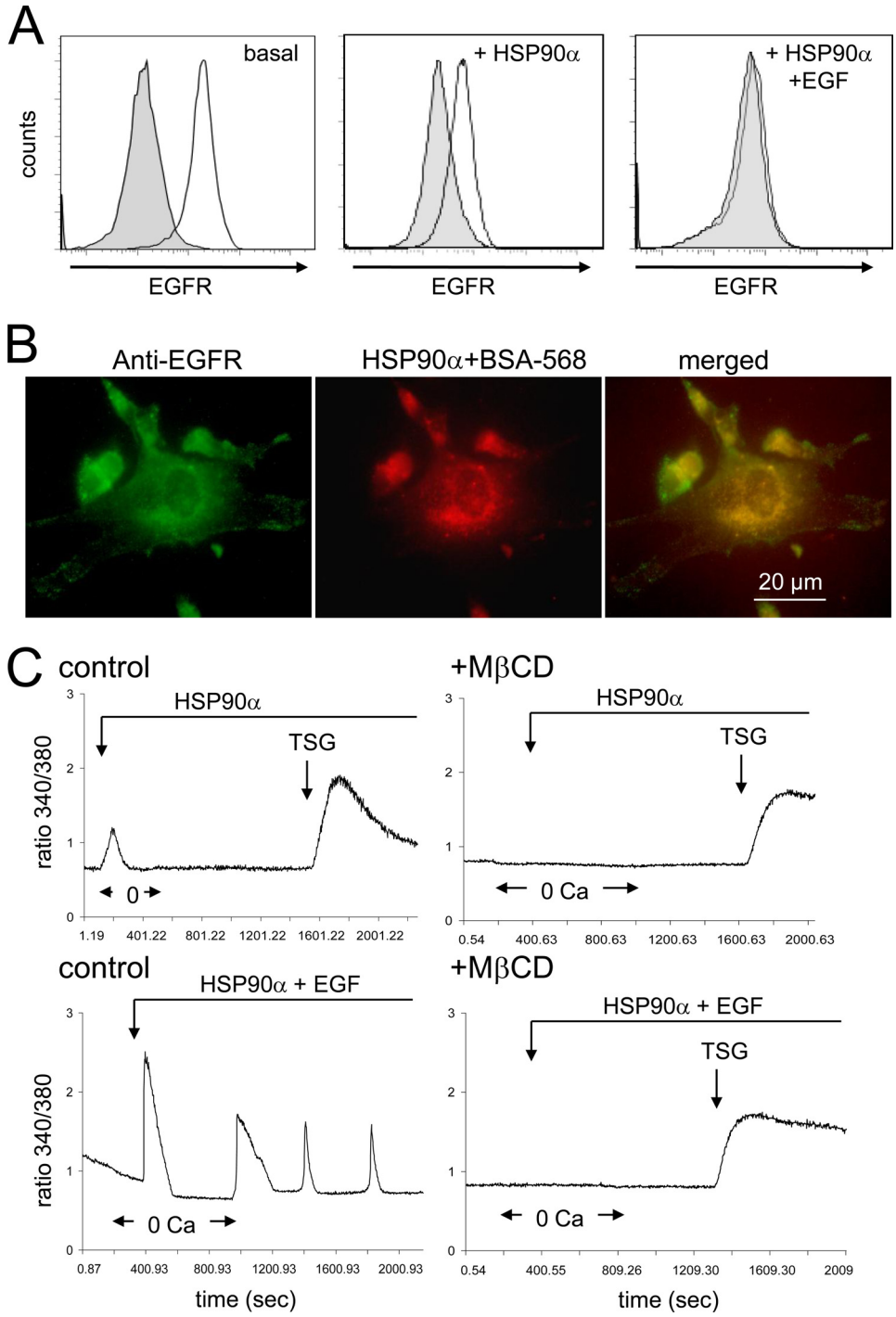

FIGURE 3. **Extracellular HSP90α induced internalization of a pool of EGFR.** *A*, flow cytometry analysis of EGFR expression in unstimulated (*basal*) and stimulated cells with 6 μg/ml HSP90α alone or with the combination of HSP90α and EGF (10 ng/ml) for 15 min. *Gray filled histograms* are isotype IgG controls. *B*, HSP90α-induced sequestration of BSA-Alexa Fluor 568 in EGFR endosomes. Cells were incubated for 15 min in HEPES-buffered saline solution containing HSP90α plus 5 μM BSA-Alexa Fluor 568 (room temperature). The *merged* panel indicates co-localization of EGFR and BSA (*yellow*; $n = 3$). *C*, raft-disrupting drug inhibits HSP90α-induced Ca^{2+} signaling. Cells pretreated with 7.5 mM MβCD for 60 min were exposed to HSP90α and/or 10 ng/ml EGF. (2 μM TSG; average of 50 cells; $n = 3$).

isozymes do not directly phosphorylate proteins at tyrosine residues, we examined the role of c-Src as an intermediate kinase between PKC and EGFR (supplemental Fig. S3). We found that the c-Src inhibitor PP2 inhibited HSP90α-induced EGFR phosphorylation, whereas its inactive form (PP3) did not. Because this EGFR transactivation was attenuated by the matrix metalloproteinase (MMP) inhibitor (GM6001) and the heparin-binding (HB)-EGF inhibitor (CRM197; see supplemental Fig. S4), MMP activation and proHB-EGF shedding slightly contribute to this process. Thus, HSP90α interacts with PKCδ, which in turn phosphorylates Src to activate EGFR.

HSP90α-induced EGFR Activation and TLR4 Signaling in U87 Cells—Extracellular HSP90α can interact with a variety of membrane receptors, including ErbB2 and TLR4 (7), and

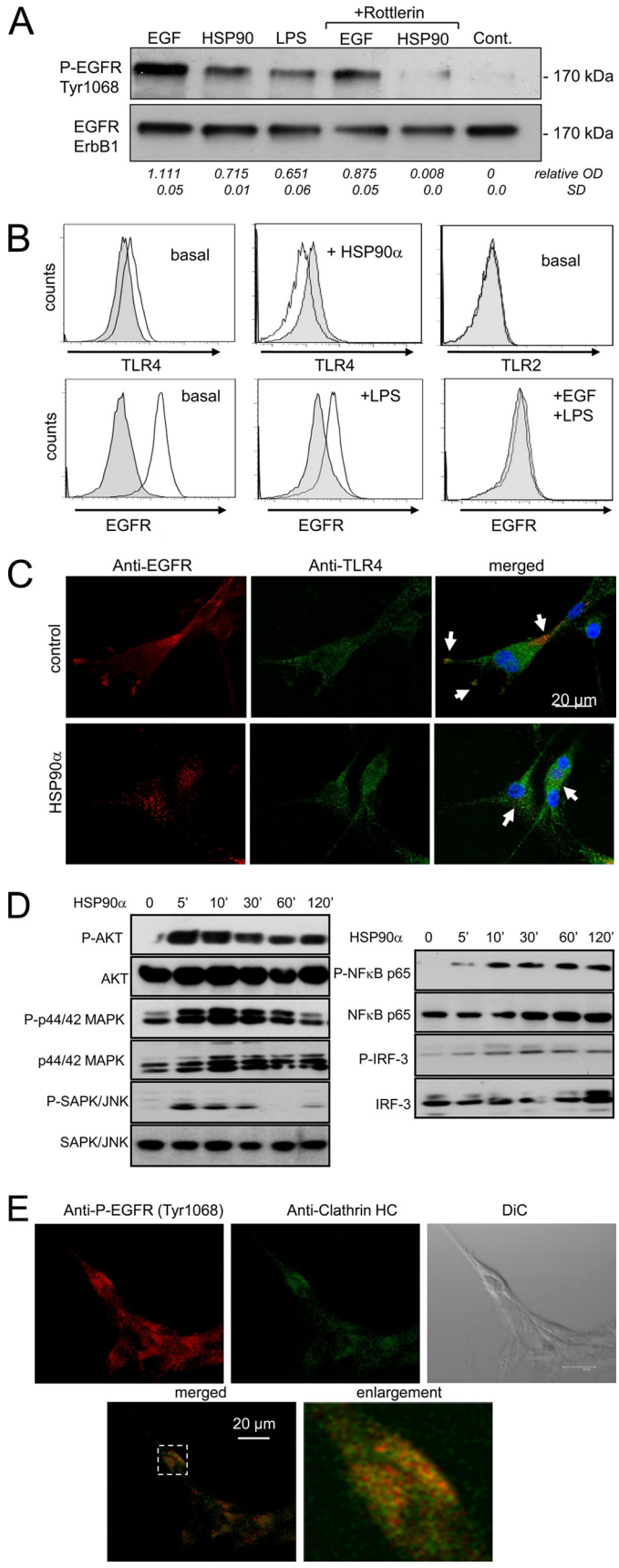

FIGURE 4. **Tyrosine phosphorylation of EGFR and partial co-localization of TLR4 and EGFR in glioblastoma cells.** *A*, extracellular HSP90α induces EGFR tyrosine phosphorylation. U87 cells were unstimulated (control (*Cont.*)) or stimulated with EGF or HSP90α and 1 μg/ml LPS for 15 min; EGFR phosphorylation at Tyr-1068 was analyzed by Western blot. In a few cases, U87 cells were pretreated for 60 min with the PKCδ inhibitor, rottlerin (10 μM). The membrane was stripped and reprobed for total ErbB1 subtype. On the bottom of the figure, values indicate the relative optical density (*OD*) of P-EGFR *versus* ErbB1 analyzed by densitometry (mean ± S.D., $n = 2$). *B*, flow cytometry analysis of cell surface expression of EGFR (ErbB1), TLR4, and TLR2 in unstimulated (*basal*) and stimulated U87 cells with HSP90α or LPS (with EGF) for 15 min. *Gray filled histograms* are isotype IgG controls ($n = 3$). *C*, U87 cells were unstimulated (control) or stimulated with HSP90α for 15 min and double-stained for TLR4 and EGFR (ErbB1). In the *merged* panel, *yellow labeling* indicates co-localization of both receptors. Confocal optical sections of 0.4 μm thickness are shown ($n = 3$). *D*, phosphorylation of Akt, p44/p42 MAPK, and SAPK/JNK (*left panel*) and of the transcription factors, NFκB p65 and IRF-3 (*right panel*). U87 cells were exposed to 6 μg/ml HSP90α for the indicated periods, and whole cell lysates were subjected to immunoblot analysis using the indicated specific antibodies recognizing phosphorylated or total forms of proteins ($n = 4$). *E*, co-localization of HSP90α-induced P-EGFR and clathrin-HC. Serum-starved U87 cells, stimulated with 6 μg/ml HSP90α for 30 min, were fixed and double-stained for the phosphorylated form of EGFR (Tyr-1068) (*red*) and the clathrin-Alexa Fluor 488 (*green*). In the *merged* panel, *yellow labeling* indicates co-localization of clathrin and P-EGFR. Confocal optical sections of 0.4 μm thickness are shown ($n = 3$). *DiC*, differential interference contrast.

TLR4 can transactivate EGFR (19). As observed for HSP90α, the bacterial LPS (1 μg/ml), a representative TLR4 ligand, also induced EGFR phosphorylation at Tyr-1068 within 15 min (Fig. 4*A*). Flow cytometry analysis indicated that TLR4 was expressed, whereas TLR2 could not be detected at the cell surface of U87 cells (Fig. 4*B*). No significant cell expression of TLR2 was shown (supplemental Fig. S5). Following external application of HSP90α, TLR4 totally disappeared at the cell surface within 15 min. Cell surface expression of EGFR was also significantly reduced on U87 cells treated with LPS. Confocal microscopy observations revealed distinct patterns of cell expression, *i.e.* EGFR was mainly located at the cell periphery, whereas TLR4 was found throughout the cell (Fig. 4*C*). However, the two receptors co-localized on the plasma membrane and concentrated in pseudopodia (or filopodia). Upon cell stimulation with HSP90α, EGFR was redistributed from the cell membrane to the juxtanuclear region where it co-localized with a small pool of internalized TLR4 (Fig. 4*C*). (Internalized EGFR by HSP90α is not targeted for degradation; see supplemental Fig. S7.) To determine the downstream signaling events of both TLR4 and EGFR activation, cells were incubated with 6 μg/ml HSP90α for 0, 5, 10, 30, 60, and 320 min (Fig. 4*D*). Phosphorylated and total AKT, p44/42 MAPK, SAPK/JNK, NFκB p65, and IRF-3 were examined by Western blot analysis. The AKT phosphorylation was induced within 5–10 min and then decreased progressively with time. The phosphorylation of p44/42 MAPK observed within 5 min reached a peak at 10 min and then returned to basal level by 6 h. The phosphorylation of SAPK/JNK also occurred rapidly within 5 min and followed a similar time course as AKT but to a lesser extent. The transcription factors, NFκB p65 and IRF-3, related to TLR4 activation, were phosphorylated within the first 10 min of HSP90α application and maintained for at least 6 h. (Intracellular calcium is required for NFκB p65 phosphorylation; see supplemental Fig. S8.) Because clathrin-mediated endocytosis is the major pathway of EGFR internalization, we also examined the co-localization of internalized receptor with clathrin-HC (heavy chain). As shown in Fig. 4*E*, P-EGFR (Tyr-1068) was internalized with

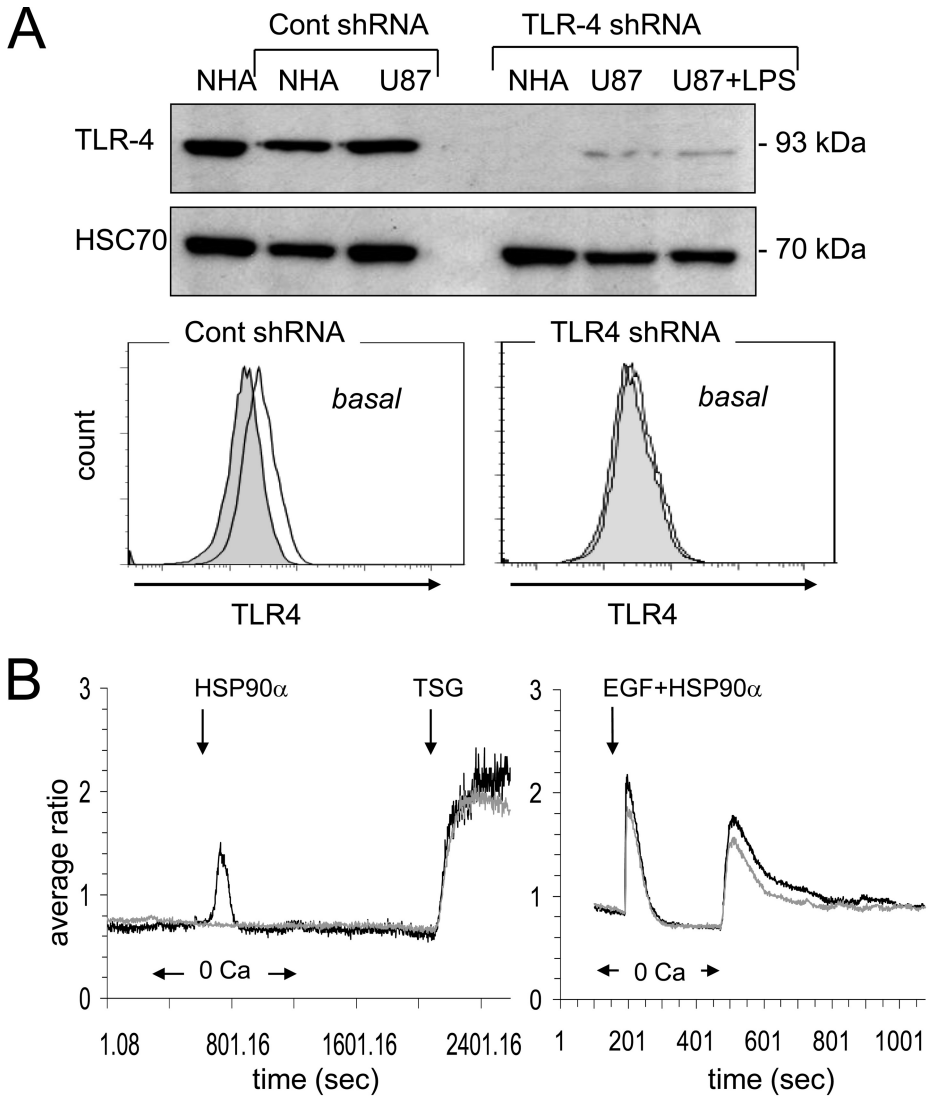

C

shRNA	control FCS-free	HSP90α	EGF	EGF HSP90α
Control COP	19,59 1,09	34,00 0,06	50,00 2,52	79,88 1,85
EGFR-shRNA	12,43 2,48*	17,25 0,46*	24,59 1,15*	28,59 1,15*
TLR4-shRNA	17,23 1,23	20,43 1,72*	52,99 2,88	71,53 1,34

FIGURE 5. **shRNA-mediated depletion of TLR4 inhibits HSP90α-induced Ca^{2+} signaling in U87 cells.** *A*, protein lysates from both normal human astrocytes (*NHA*) and glioblastoma U87 cells were probed with anti-TLR4 (HSC70 as loading control). TLR4 expression in normal human astrocytes and U87 cells was shown, and cell stimulation with 1 μg/ml LPS for 60 min was performed. Flow cytometry analysis of TLR4 expression in transfected U87 cells (*white histogram*) when compared with IgG control (*gray filled histogram*; $n = 3$) as performed. *B*, effects of HSP90α, LPS (1 μg/ml), TSG (2 μM), and HSP90α plus EGF on $[Ca^{2+}]_i$ in TLR4 shRNA (*grey curves*) and control shRNA (*black curves*) transfected U87 cells (average of 6 cells; $n = 3$). *C*, consequences of shRNA-mediated depletion of TLR4 and EGFR (ErbB1) onto the cell invasion. The quantitative effect of HSP90α (6 μg/ml) and/or EGF (10 ng/ml) on the closure of wound after a 12-h treatment is depicted in the table (mean ± S.D., $n = 2$; *, p values<0.05 *versus* control). The following cells were used as control in this specific experiment; cultures of U87 cells and normal human astrocytes (Lonza Walkersville, Inc.) were grown to confluency in DMEM plus 10% fetal bovine serum (Lonza). For lentiviral transduction particles and transfections, human TLR4 shRNA, EGFR (ErbB) shRNA and control lentiviral particles were used according to the manufacturer's recommendations (Santa Cruz Biotechnology).

clathrin after 30 min of cell stimulation with HSP90α. No co-localization with P-EGFR and caveolin-1 was observed (data not shown). Furthermore, chlorpromazine, a well known inhibitor of clathrin-mediated endocytosis, significantly blocked the internalization of P-EGFR and the MAPK signaling induced by HSP90α (see supplemental Fig. S6). Thus, clathrin-mediated internalization is essential for a sustained HSP90α-mediated EGFR signaling. Because cholesterol depletion by MβCD also blocks calcium signaling and endocytic processes, our findings support the view that HSP90α-induced endocytosis recruits at least two kinds of membrane rafts: one including TLR4 and the second including EGFR. Altogether, our data suggest that signaling via the PKCδ/c-Src pathway is involved in

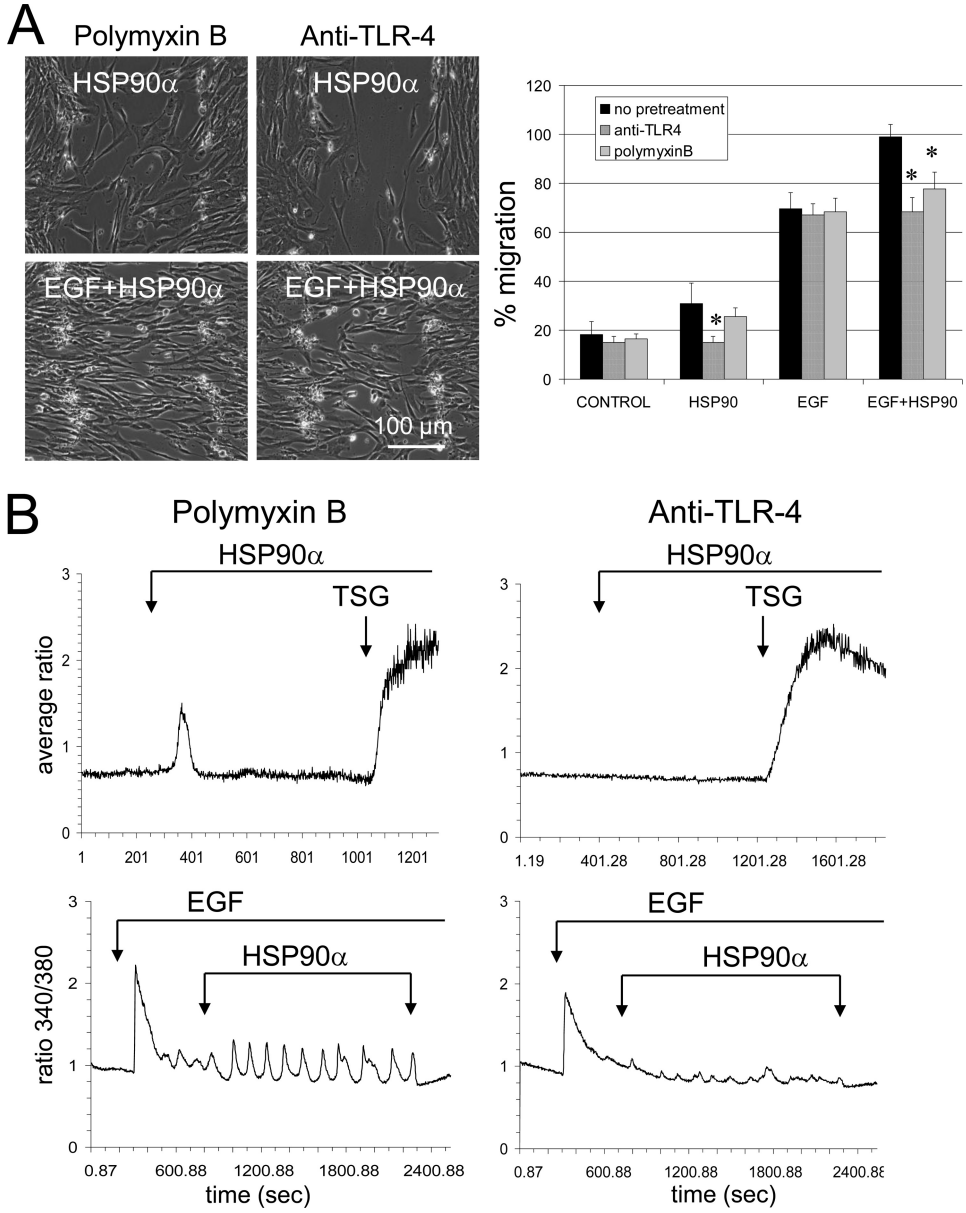

FIGURE 6. **The HSP90α-induced cell migration and Ca^{2+} signaling are slightly reduced by an endotoxin-binding agent but totally abolished by blocking TLR4.** *A*, wound healing assay in U87 cell cultures. Cells were pretreated with Polymyxin B (10 μM, 60 min) or a blocking anti-TLR4 antibody (10 μg/ml, 30 min). *Upper* and *lower panels*, phase-contrast images obtained at 11 h after scratch formation in the presence of HSP90α (*upper panels*) or HSP90α plus EGF (*lower panels*). Quantitative effects on the closure of wound are depicted in the histogram (mean ± S.D., $n = 3$; *, p values<0.05 *versus* control). *B*, fura-2 intracellular Ca^{2+} imaging of U87 cells in response to HSP90α and/or EGF stimulation, plus TSG 2 μM as indicated by *arrows* ($n = 3$).

HSP90α-induced EGFR transactivation, upstream of EGFR tyrosine phosphorylation.

TLR-4 Is Required for HSP90α-induced $[Ca^{2+}]_i$ Rise—Down-regulation of TLR4 using a lentivirus encoding a specific shRNA (Fig. 5*A*) abolished the Ca^{2+} response to HSP90α and LPS but did not affect the TSG-induced increase in $[Ca^{2+}]_i$ (Fig. 5*B*). This down-regulation induced a significant reduction in both the release of internal Ca^{2+} stores and the secondary external Ca^{2+} influx in response to EGF plus HSP90α. Thus, TLR4 may be required for HSP90α-induced $[Ca^{2+}]_i$ increase in U87 cells. The contribution of TLR4 and EGFR (ErB1) to HSP90α-mediated cell invasion is shown in Fig. 5*C*. In shRNA-mediated knockdown of TLR4 or EGFR, the cell migration was severely impaired in response to HSP90α. Thus, in agreement with our previous results, TLR4 is required for HSP90α effects. To rule out a role of contamination of recombinant HSP90α with LPS, cells were preincubated with Polymyxin B, an endotoxin-binding agent (10 μM; 30–60 min). HSP90α without contaminant LPS was always able to amplify the EGF-induced cell migration (Fig. 6*A*). This cell pretreatment reduced but did not inhibit HSP90α-induced transient rise in $[Ca^{2+}]_i$ (Fig. 6*B*, *left panels*). Preincubation of U87 cells with anti-TLR4-blocking antibody (27) abolished the increase in $[Ca^{2+}]_i$ and the cell migration induced by HSP90α (Fig. 6, *right panels*) and decreased EGF-induced cell responses (Fig. 6, *right panels*). Altogether, HSP90α, through a direct or indirect activation of TLR-4, upregulates EGF-induced cell responses.

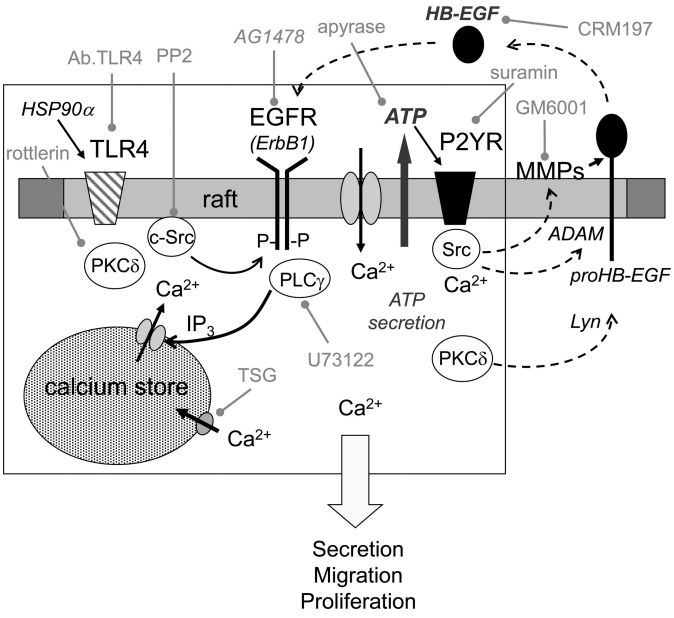

FIGURE 7. **Hypothetic scheme representation of the signaling pathways involved in HSP90α-induced transactivation of EGFR at Tyr-1068 through TLR4 in glioblastoma U87 cell line.** Our data are summarized in the *box* and linked to pathways (*outside the box*) previously proposed by other authors for cell migration. Specific inhibitors used in this work are written in *grey*. Upon HSP90α stimulation of TLR4, PKCδ phosphorylates c-Src to activate EGFR in rafts. Assemblage of EGFR, c-Src, and phospholipase Cγ (*PLC*γ) might form a platform for the EGFR, resulting in the release of ATP from U87 cells. The released ATP, through its P2 receptors, triggers intracellular Ca^{2+} waves, leading to the activation of ADAM protein(s), which cleaves pro-HB-EGF at the cell surface. HB-EGF in an autocrine and/or paracrine fashion binds EGFR, amplifying signals into the intracellular signaling network. The initial activation of PKCδ could also involve Lyn, MMP2/9, and HB-EGF release.

DISCUSSION

Cell surface expression of HSP90α has been associated in various tumor types to their migration capabilities and metastatic potential (5–8). Here, we show in glioblastoma U87 cell line that extracellularly applied HSP90α activates a signal transduction pathway involving TLR4 to amplify the effects of EGF on cell shape and cell migration. More specifically, extracellular HSP90α triggers EGFR phosphorylation at Tyr-1068 through a pathway that can be inhibited by rottlerin and PP2, suggesting a role of PKCδ and c-Src (Fig. 7). Extracellular HSP90α also transiently increases cytosolic $[Ca^{2+}]$ in U87 cells and converts calcium response induced by EGF from a transient to an oscillatory pattern. Ca^{2+} mobilization induces ATP release that amplifies the cell response through a suramin-inhibited pathway. Altogether, these results identify the additive effect of extracellular HSP90α and EGF on glioma cell migration capabilities in human brain tumors.

TLR4-mediated transactivation of EGFR has been identified in epithelial cells (8, 19). For example, this receptor cross-talk has been observed in response to *Helicobacter pylori* protein in gastric cells (19). Here, we show that extracellular HSP90α can induce TLR4-mediated EGFR transactivation and its downstream effects, *i.e.* cell migration and Ca^{2+} signaling, in U87 cells. Furthermore, shRNA-mediated down-regulation of TLR4 or its neutralization with a specific antibody prevents HSP90α-induced activation of EGFR. Co-localization of EGFR, TLR4-ligand complexes, and extracellular HSP90α in specific membrane domains could favor an interaction between TLR4 and EGFR that would allow EGFR activation. Depletion of cholesterol by methyl-β-cyclodextrin disrupted this co-localization and impaired HSP90α-induced Ca^{2+} rise, even in the presence of EGF. MβCD could prevent the activation of PKCδ, Src, and Lyn kinases, as demonstrated in other cell types (19, 28, 29). Interestingly, EGFR and TLR4 were observed to co-localize in pseudopodia or filopodia of non-stimulated glioblastoma cells whose polarization and stabilization determines cell motility (30). Upon cell exposure to HSP90α, EGFR and TLR-4 were rapidly internalized with kinetics similar to that induced by their respective ligands, EGF and LPS.

HSP90α appears to trigger EGFR transactivation through a pathway that is sensitive to both PKCδ and c-Src inhibitors (Fig. 7). Because PKC isozymes do not directly phosphorylate proteins at tyrosine residues, c-Src would be an intermediate kinase between PKCδ and EGFR (35, 38). The expression and activity of PKC isozymes are highly elevated in gliomas and glioma cell lines (31–33), and PKC inhibitors markedly reduce glioma cell proliferation (34). PKCδ isoform was shown to phosphorylate several kinases including c-Src (35), ADAM, and Lyn (36). Cellular Src and EGFR act synergically to facilitate the progression of human brain tumors (35, 37, 38), whereas ADAM and Lyn kinases regulate activation of MMPs, proHB-EGF shedding, and EGFR tyrosine phosphorylation (20, 36). Inhibition of extracellular HSP90α was shown to decrease MMP-2 activity, blocking invasiveness (8). The EGFR (ErbB1) kinase inhibitor, AG1478, only attenuated HSP90α-induced transactivation of EGFR at Tyr-1068 in U87 cells, at a dose known to completely abrogate EGF-induced phosphorylation of EGFR. This suggests that HSP90α-induced EGFR Tyr-1068 phosphorylation through PKCδ and c-Src is upstream of EGFR kinase activity. This result agrees with similar studies that used phorbol 12-myristate 13-acetate to transactivate the EGFR (35).

Intracellular Ca^{2+} modulates the proliferative effects of EGF (16, 39, 40), and complex Ca^{2+} oscillations are associated with human astrocytoma cell migration (25, 41, 42). A major component of Ca^{2+} homeostasis is the ER, which stores micromolar levels of Ca^{2+} under control of Ca^{2+}-ATPases known as sarcoplasmic reticulum Ca^{2+}-ATPase (SERCAs), which maintain a low cytosolic $[Ca^{2+}]$. Specific inhibition of sarcoplasmic reticulum Ca^{2+} ATPase activity with TSG results in ER Ca^{2+} depletion and consequent opening of store-operated calcium channels located in the plasma membrane. These channels elevate cytosolic $[Ca^{2+}]$, and under physiological conditions, permit refilling of the ER Ca^{2+} pool. The magnitude of the increase in $[Ca^{2+}]_i$ evoked by an agonist is thus dependent on the size of stores, leakiness of the ER membrane for Ca^{2+}, and activity of store-operated calcium channels. Here, we show that extracellular HSP90α transiently increases cytosolic $[Ca^{2+}]$ in glioblastoma U87 cells and converts calcium response induced by EGF from a transient to an oscillatory pattern. Similar calcium oscillations induced by EGF have been previously reported in astrocytes in response to glutamate (42), pro-inflammatory cytokines (41), or thimerosal, which directly activates the inositol 1,4,5-

triphosphate receptor and induces calcium release from internal stores (43). These stimuli also induce release of ATP by astrocytes. Elevation of cytosolic Ca^{2+} is a major regulator of nucleotide export in astrocytes, either by channel-mediated influx or through vesicle exocytosis. Rho activation and other changes in cytoskeletal organization have also been implicated in ATP release (44). Here, we show an elevated cytosolic Ca^{2+} and an increase in F-actin content by stimulation of EGFR in U87 cells (supplemental Fig. S1). Stimulation of EGFR was reported to activate RhoA/Rho-associated protein kinase signaling, which could synergize with Ca^{2+} mobilization to induce ATP release in response to HSP90α plus EGF.

Altogether, our data indicate that the ability of extracellular HSP90α to increase cytosolic [Ca^{2+}] in tumoral astrocytes and to induce complex Ca^{2+} oscillations in the concomitant presence of EGF probably facilitates the migration of these cells. It remains to be demonstrated whether amplification of this pathway in tumor cells accounts for the relationship established between extracellular HSP90α and tumor cell invasion and metastasis formation.

Acknowledgments—We are grateful to Dr. Anne-Marie LeBon (UMR Flavic, Institut National de la Recherche Agronomique (INRA) Dijon) and Christine Arnould for confocal microscopy (CMSE, INRA Dijon). This work has been benefited from the facilities and expertise of the photonic imagery platform of IMAGIF (Centre de recherché de Gif). We thank Marie-Noëlle Soler for expert support with confocal microscopy.

REFERENCES

1. Schwartzbaum, J., Ahlbom, A., Malmer, B., Lönn, S., Brookes, A. J., Doss, H., Debinski, W., Henriksson, R., and Feychting, M. (2005) *Cancer Res.* **65,** 6459–6465
2. Kleihues, P., and Ohgaki, H. (2000) *Toxicol. Pathol.* **28,** 164–170
3. Bian, X. W., Chen, J. H., Jiang, X. F., Bai, J. S., Wang, Q. L., and Zhang, X. (2004) *Int. Immunopharmacol.* **4,** 1537–1547
4. Scott, J. N., Rewcastle, N. B., Brasher, P. M., Fulton, D., Hagen, N. A., MacKinnon, J. A., Sutherland, G., Cairncross, J. G., and Forsyth, P. (1998) *Can. J Neurol. Sci.* **25,** 197–201
5. Becker, B., Multhoff, G., Farkas, B., Wild, P. J., Landthaler, M., Stolz, W., and Vogt, T. (2004) *Exp. Dermatol.* **13,** 27–32
6. Sidera, K., Samiotaki, M., Yfanti, E., Panayotou, G., and Patsavoudi, E. (2004) *J. Biol. Chem.* **279,** 45379–45388
7. Sidera, K., Gaitanou, M., Stellas, D., Matsas, R., and Patsavoudi, E. (2008) *J. Biol. Chem.* **283,** 2031–2041
8. Eustace, B. K., Sakurai, T., Stewart, J. K., Yimlamai, D., Unger, C., Zehetmeier, C., Lain, B., Torella, C., Henning, S. W., Beste, G., Scroggins, B. T., Neckers, L., Ilag, L. L., and Jay, D. G. (2004) *Nat. Cell Biol.* **6,** 507–514
9. Yang, Y., Rao, R., Shen, J., Tang, Y., Fiskus, W., Nechtman, J., Atadja, P., and Bhalla, K. (2008) *Cancer Res.* **68,** 4833–4842
10. Tsutsumi, S., and Neckers, L. (2007) *Cancer Sci.* **98,** 1536–1539
11. Tsutsumi, S., Scroggins, B., Koga, F., Lee, M. J., Trepel, J., Felts, S., Carreras, C., and Neckers, L. (2008) *Oncogene* **27,** 2478–2487
12. Webb, D. J., Parsons, J. T., and Horwitz, A. F. (2002) *Nat. Cell Biol.* **4,** E97–100
13. Libermann, T. A., Nusbaum, H. R., Razon, N., Kris, R., Lax, I., Soreq, H., Whittle, N., Waterfield, M. D., Ullrich, A., and Schlessinger, J. (1985) *Nature* **313,** 144–147
14. Ekstrand, A. J., Sugawa, N., James, C. D., and Collins, V. P. (1992) *Proc. Natl. Acad. Sci. U.S.A.* **89,** 4309–4313
15. van der Geer, P., Hunter, T., and Lindberg, R. A. (1994) *Annu. Rev. Cell Biol.* **10,** 251–337
16. Climent, E., Sancho-Tello, M., Miñana, R., Barettino, D., and Guerri, C. (2000) *Neurosci. Lett.* **288,** 53–56
17. Nishikawa, R., Ji, X. D., Harmon, R. C., Lazar, C. S., Gill, G. N., Cavenee, W. K., and Huang, H. J. (1994) *Proc. Natl. Acad. Sci. U.S.A.* **91,** 7727–7731
18. Riese, D. J., 2nd, and Stern, D. F. (1998) *Bioessays* **20,** 41–48
19. Basu, S., Pathak, S. K., Chatterjee, G., Pathak, S., Basu, J., and Kundu, M. (2008) *J. Biol. Chem.* **283,** 32369–32376
20. Bergin, D. A., Greene, C. M., Sterchi, E. E., Kenna, C., Geraghty, P., Belaaouaj, A., Taggart, C. C., O'Neill, S. J., and McElvaney, N. G. (2008) *J. Biol. Chem.* **283,** 31736–31744
21. Barabé, F., Paré, G., Fernandes, M. J., Bourgoin, S. G., and Naccache, P. H. (2002) *J. Biol. Chem.* **277,** 13473–13478
22. Asea, A., Rehli, M., Kabingu, E., Boch, J. A., Bare, O., Auron, P. E., Stevenson, M. A., and Calderwood, S. K. (2002) *J. Biol. Chem.* **277,** 15028–15034
23. Tsan, M. F., and Gao, B. (2004) *Cell Mol. Immunol.* **1,** 274–279
24. Tsan, M. F., and Gao, B. (2009) *J Leukoc. Biol.* **85,** 905–910
25. Bryant, J. A., Finn, R. S., Slamon, D. J., Cloughesy, T. F., and Charles, A. C. (2004) *Cancer Biol. Ther.* **3,** 1243–1249
26. Bowser, D. N., and Khakh, B. S. (2007) *J Gen. Physiol.* **129,** 485–491
27. Blanco, A. M., Vallés, S. L., Pascual, M., and Guerri, C. (2005) *J. Immunol.* **175,** 6893–6899
28. Hur, E. M., Park, Y. S., Lee, B. D., Jang, I. H., Kim, H. S., Kim, T. D., Suh, P. G., Ryu, S. H., and Kim, K. T. (2004) *J. Biol. Chem.* **279,** 5852–5860
29. Hsieh, H. L., Tung, W. H., Wu, C. Y., Wang, H. H., Lin, C. C., Wang, T. S., and Yang, C. M. (2009) *Arterioscler. Thromb. Vasc. Biol.* **29,** 1594–1601
30. Jia, Z., Barbier, L., Stuart, H., Amraei, M., Pelech, S., Dennis, J. W., Metalnikov, P., O'Donnell, P., and Nabi, I. R. (2005) *J. Biol. Chem.* **280,** 30564–30573
31. Couldwell, W. T., Antel, J. P., and Yong, V. W. (1992) *Neurosurgery* **31,** 717–724
32. Baltuch, G. H., and Yong, V. W. (1996) *Brain Res.* **710,** 143–149
33. Bredel, M., and Pollack, I. F. (1997) *Acta Neurochir.* (*Wien.*) **139,** 1000–1013
34. Hussaini, I. M., Karns, L. R., Vinton, G., Carpenter, J. E., Redpath, G. T., Sando, J. J., and VandenBerg, S. R. (2000) *J. Biol. Chem.* **275,** 22348–22354
35. Amos, S., Martin, P. M., Polar, G. A., Parsons, S. J., and Hussaini, I. M. (2005) *J. Biol. Chem.* **280,** 7729–7738
36. Zhao, Y., He, D., Saatian, B., Watkins, T., Spannhake, E. W., Pyne, N. J., and Natarajan, V. (2006) *J. Biol. Chem.* **281,** 19501–19511
37. Biscardi, J. S., Maa, M. C., Tice, D. A., Cox, M. E., Leu, T. H., and Parsons, S. J. (1999) *J. Biol. Chem.* **274,** 8335–8343
38. Biscardi, J. S., Tice, D. A., and Parsons, S. J. (1999) *Adv. Cancer Res.* **76,** 61–119
39. Tu, M. T., Luo, S. F., Wang, C. C., Chien, C. S., Chiu, C. T., Lin, C. C., and Yang, C. M. (2000) *Br. J. Pharmacol.* **129,** 1481–1489
40. Rondé, P., Giannone, G., Gerasymova, I., Stoeckel, H., Takeda, K., and Haiech, J. (2000) *Biochim. Biophys. Acta* **1498,** 273–280
41. Morita, M., Higuchi, C., Moto, T., Kozuka, N., Susuki, J., Itofusa, R., Yamashita, J., and Kudo, Y. (2003) *J. Neurosci.* **23,** 10944–10952
42. Morita, M., Kozuka, N., Itofusa, R., Yukawa, M., and Kudo, Y. (2005) *J. Neurochem.* **95,** 871–879
43. Swann, K. (1991) *FEBS Lett.* **278,** 175–178
44. Blum, A. E., Joseph, S. M., Przybylski, R. J., and Dubyak, G. R. (2008) *Am. J. Physiol. Cell Physiol.* **295,** C231–C241